A Polymer Physics Perspective on why PEI is an Effective Non-Viral Gene Delivery Vector

Caleb Gallops, Jesse Ziebarth, Yongmei Wang*

Department of Chemistry, The University of Memphis, Memphis, Tennessee 38154, United States

*Corresponding author: ywang@memphis.edu

Polyethyleneimine (PEI) was the first polycation that was shown to have a high transfection efficiency among non-viral gene delivery vectors. The high transfection efficiency was attributed to the proton sponge effect due to the partially protonated amines on PEI chains. Although the proton sponge effect has been debated, here we provide a look at PEI structure and dynamics from polymer physics perspective. We discuss the protonation equilibrium on PEI chains, the conformational change of PEI chains, and the ion condensation on PEI chains. These three processes can all act favorably to the release of nucleic acids from endosome, thus lead to high transfection efficiency. These three processes all stem from the unique chemical structure of PEI, exemplifying how chemical structure determines property.

Introduction

The search for non-viral based gene delivery vectors began in the last century when the potential of gene therapy to treat various diseases became recognized.[1] The interest in non-viral based delivery vectors increased when patients who received gene therapy developed unpredictable immune responses due to the use of viral-based delivery vectors.[2] The choices of non-viral based delivery methods include gene-gun (forcing the genetic materials into cells through hydrodynamic force), cationic lipids and cationic polymers.[3] Among these three broad areas, polymer based delivery vectors attracted the most attention since polymers offer versatility to be modified/synthesized in terms of their chemical and physical properties.[4–6] Polyethyleneimine (PEI) was reported to be a versatile vector for gene and oligonucleotide transfer into cells *in vitro* and *in vivo* in 1995.[7] Other forms of cationic polymers have also been tested for their ability to transfer nucleic acids into cells,[8–14] but PEI became the gold standard for measuring the transfection efficiency of non-viral based gene delivery vectors. PEI is traditionally prepared by ring opening polymerization of aziridine, which leads to branched structures that contain the primary amines at the end, secondary amine along the chain and tertiary amine at the branch points.[15] Linear form of PEI (lPEI) can be obtained by hydrolysis of acyl groups after the ring opening polymerization of *N*-substituted oxazoline.[16,17] Reaching quantitative hydrolysis however is challenging and it was only within this decade that lPEI became widely available after concerted effort to improve the synthesis conditions for lPEI.[17]

PEI has some unique structural characteristics compared with other cationic polymers. While all cationic polymers bear amine groups, most cationic polymers carried the amine groups on the side chain such as polylysine (PLL) or poly (2-(dimethylamino)ethyl methacrylate) (pDMAEMA), PEI, however, bears the amine groups on the backbone of the chain. Moreover, the two amine groups are separated only by two methylene groups, leading to proximity of the two amine groups. This unique arrangement of the amine groups in PEI chains led to the proton sponge hypothesis[7,18] that attributes the high transfection efficiency of PEI-mediated delivery of nucleic acids to the buffering capacity of PEI in endosome. According to the proton sponge hypothesis, this buffering capacity of PEI is thought to cause an increase in ATPase pumping of H^+ inside the endosome as well as passive Cl^- entry into the endosome, forcing the endosome to rupture due to high osmotic pressure and allowing PEI/nucleic acid polyplexes to escape from endosome. This hypothesis has been debated and refined over an extensive amount of studies.[19,20,29–35,21–28] These refinements suggest that, in addition to the above osmotic rupture mechanism, the cationic PEI chains interact with the phospholipid membrane of the endosome, resulting in the permeabilization of the membrane and facilitating the release of polyplex from the endosome.[36] While the actual cellular mechanism of PEI actions during the transfection needs to be investigated within the context of cellular processes, there are some unique physical and chemical properties of PEI chains that could impact the PEI-mediated nucleic acid deliveries. Here we provide a discussion on the unique physical and chemical properties of linear PEI chains and show how these unique properties may play roles in PEI-mediated transfection of nucleic acids.

Protonation of Diamines

While the pK_a for the conjugated acid of a single amine group is measured to be around 10.5 for a primary amine or 10.7 for a tertiary amine, the protonation of diamines become stepwise and two pK_as can be defined based on titration curves. The two pK_as for diamines separated by two, three or more methylene groups has been reviewed and summarized by Bencini et al.[37] The pK_a shift, shown as difference in the two pK_as, $\Delta pK_a = pK_{a1} - pK_{a2}$ will have one of the pK_as downshifted, while the first one remains around 10.5. Figure 1 presents the plot of ΔpK_a as a function of number methylene group between the two amines. The amount of shift in ΔpK_a can be traced to an additional cost of free energy when the two pronated amines were close by. Assuming the additional cost of free energy ΔG is purely electrostatic interaction through space, one may write this ΔG as

$$\Delta G = \frac{q_i q_j \exp(-\kappa r_{ij})}{4\pi\epsilon_0\epsilon_r r_{ij}} = q_i q_j W_{elec}(r_{ij}) \quad (1)$$

where r_{ij} is the distance between the two charged amine groups, κ^{-1} is the Debye length, ε_r is the relative dielectric constant of the medium. Additionally, the shift in measured difference in macroscopic ΔpK_a is related to ΔG through:

$$\Delta pK_a = \frac{\Delta G}{2.303 k_B T} + \log_{10} 4 \quad (2)$$

The numeric $\log_{10}(4)$ is needed to account for the statistics of the microstates.[38] Figure 1 presents the experimentally reported ΔpK_a for the diamines as a function of number of carbon atoms as reported by Bencini et al (symbols), along with the theoretical prediction[38] according to Eqs (1) and (2) using the measured distance r between diamines using molecular models and by assuming ionic strength I=0.1M, same as with experimental conditions. One caveat in the above theoretical investigation is that the dielectric constant ε_r used is not 78.0, as normally assumed for water, instead a distance dependent dielectric constant expression was used. The validity of such an approach is certainly worth further investigation, but this approximation allows one to consider the protonation of polyethyleneimine, which contains multiple amine groups located on the chain.

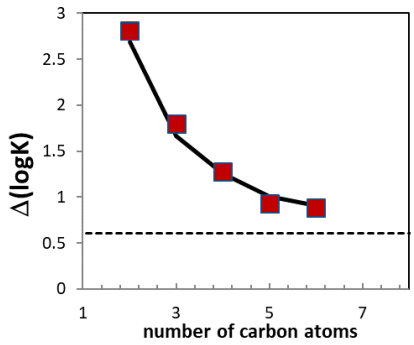

Figure 1: The difference in two p*K*a's for the diamines separated by different number of carbon atoms. The symbols are experimental data reported in Bencini et al. The horizontal dashed line shows the limit of Δp*K* due to statistic effect when the additional cost of free energy of ionization becomes zero. The solid line is the calculated Δp*K* according to Equations (1) and (2) by using the distance *r* measured in molecular models.[38]

Protonation of PEI Chains

The protonation equilibrium of a single amine is described by Henderson-Hasselbalch equation, and normally it will be protonated at pH=7 with its intrinsic pK_a =10.5. However, the amines on a PEI chain are not all protonated at pH=7 because of this electrostatic interaction between charged groups. The fraction of sites that are protonated/deprotonated in a PEI chain is best studied by developing a multisite Monte Carlo titration model.[38] During the Monte Carlo titration, an amine site j is randomly selected to switch the protonation state. Each switch is associated with a change of free energy according to the following equation and the switch is accepted or rejected according to the Metropolis rule.

$$\Delta E = \pm 2.303 k_B T\,(pH - pK_0) + \sum_i q_i q_j W_{elec}(r_{ij}) \qquad (3)$$

The plus and minus sign is associated with protonation and deprotonation respectively and pK_0 is the intrinsic pK_a of a single amine site. This Monte Carlo titration step is performed together with regular Monte Carlo moves of a coarse-grained linear PEI chain where the chain is subjected to conformational changes. By doing so, we have effectively taken care of the coupling between the protonation/deprotonation process and the conformational change of PEI. We were able to obtain the "typical" protonation states of a linear PEI at a given pH and compared our computational titration curve with experimentally reported ones (see Figure 2). The agreement between theory and experiment was good, but some disagreement in salt concentration dependence were observed. The disagreement could be traced to the use of screened electrostatic interaction term. A significant result emerges from such comparison is that at physiological pH=7, there is about 40% to 50% amines protonated depending on salt concentrations. The theoretical investigation undertook by us provide the support that PEI chain has the buffering capacity as there are many amines on PEI chains not protonated at pH=7. These amine sites are capable of picking up more protons when pH is lowered.

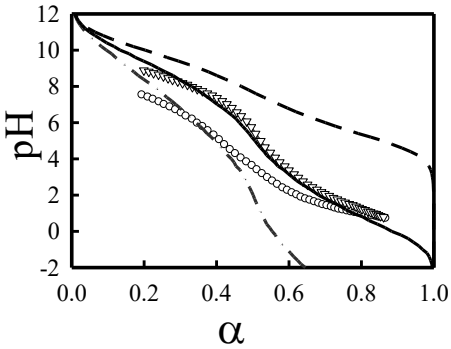

Figure 2: Overlay of experimental titration curves from Smits et al.[39] (shown in symbols) with computational titration curves (shown as lines) with distance dependent dielectric model. The salt concentrations for experimental curves Cs = 0M (circles) and 0.1M (triangles). Salt concentrations for computational titration curves are Cs = 0M (dot-dashed line), 0.01M (solid line), and 0.1M (dashed line). pK_0 was assumed to be 10.0 in computational titration curves. Reproduced with permission from reference [38]. Copyright [2010], American Chemical Society.

Conformational Change of PEI Chain at different pH

When the level of protonation in the PEI changes, the chain undergoes a dramatic conformational change. Experimental studies of this conformational change is challenged by aggregations between the chains.[40] We used the atomistic molecular dynamic simulations and simulated a linear PEI chain with 40-repeating unit with level of protonation systematically changed from 0% to 100%.[41] The PEI chain is immersed in water (modeled as TIP3P) with counter ions and additional monovalent NaCl salts as desired. Figure 3 is a visual representation of the PEI chain at five different protonation levels after the chain reaches equilibrium in simulations. The chain changes from a collapsed globule conformation to a rod-like conformation. This conformational change is achieved through the change of torsional angle, defined by N-C-C-N, from a primarily *gauche*+/- state to a *trans* state. The distance between the two neighboring amines, L_0, measured from nitrogen atom to the next nitrogen atom (regardless if they are protonated or not) also experience an increase from 3.1Å to 3.9 Å (see Figure 4).

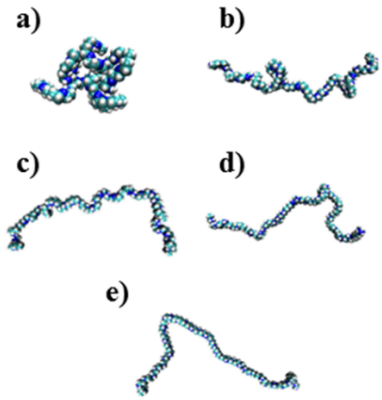

Figure 3: Visualizations of PEI chains for the fraction of protonated amines α: (a) α = 0, (b) α = 0.25, (c) α = 0.5, (d) α = 0.75 and (e) α = 1.0. In order to see monomeric structure of the chain, the images are not to scale. Reproduced with permission from reference [41]. Copyright [2019], American Chemical Society .

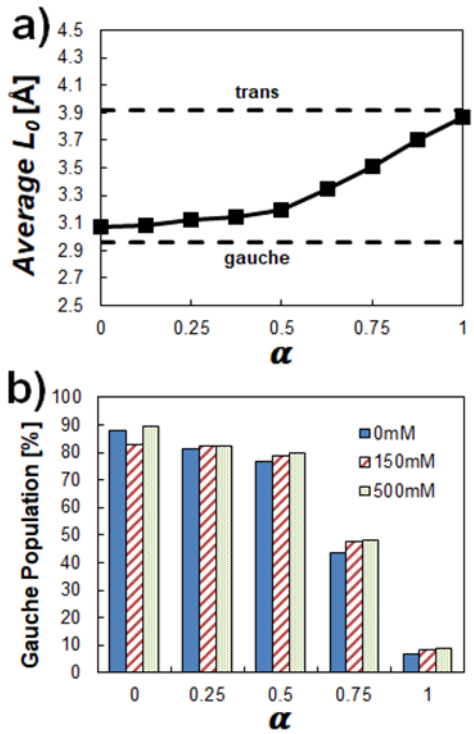

Figure 4: Panel (a) is the average length between neighboring amines L_0; Panel (b) is the population of torsional angle (defined by N-C-C-N) in gauge state. The legend in panel (b) is the salt concentrations. All data are obtained from molecular dynamic simulations of a single PEI chain. Adapted with permission from reference [41]. Copyright [2019], American Chemical Society .

It is evident from Figure 4 that there is an abrupt change when the fraction of charged amines α exceeds 50%. Before that, the change in the length L_0 and gauge populations are gradual. A further examination of the chain conformation by looking into the persistent length L_p, radius of gyration of chain R_g, and end-to-end vector R reveals that indeed one may divide the conformational transition to two regimes, a weakly charged regime, and a strongly charged regime (Figure 5). During the weakly charged regime, the persistent length L_p remains low, the chain is essentially flexible, however, R_g and R both increase quite dramatically as α increases. In the highly charged regime, however, the persistent length L_p increases noticeably, accompanied by further increase in R_g and R. The increase in R_g and R in the highly charged regime can be accounted for by the increase in L_p according to Worm-Like-Chain model (WLC).[42] However, the increase in R_g and R in the weakly charged regime does not fit the WLC model. The conformational change in the weakly charged regime is due to breaking of hydrophobic attraction within the chain.

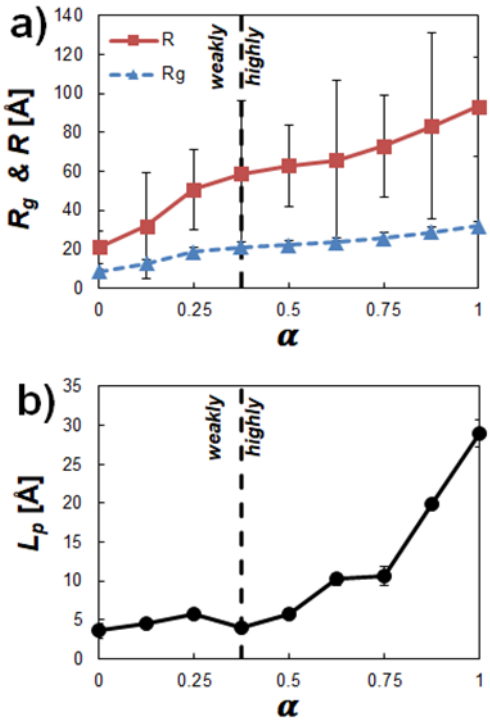

Figure 5: Change in (a) radius of gyration R_g ((triangles) and end-to-end distance R (squares) and (b) persistence length L_p for a single PEI chain with 40 repeating units as a function of protonation level, α, for simulations in salt-free conditions. Reproduced with permission from reference [41]. Copyright [2019], American Chemical Society.

Ion Condensation around PEI Chain at Highly Charged Regime

Ion condensation is a phenomenon well-known in polyelectrolyte. We begin with the definition of the Bjerrum length l_B: the distance at which Coulombic potential between two unit charges equals to the thermal energy.

$$k_B T = \frac{e^2}{4\pi\epsilon_o\epsilon_r l_B} \qquad (4)$$

The Bjerrum length in aqueous water is about 7.1 Å. Recall that the nearest amine-to-amine distance L_0 is around 3.1Å to 3.9 Å (see Figure 3), therefore if two neighboring amines are both protonated (formation of doublet), then the charge-to-charge distance will be smaller than Bjerrum length. In discussions of polyelectrolyte theory, it was recognized that if one defines a dimensionless parameter, $\Gamma = l_B/A$, where A is the distance between neighboring charged units, then when $\Gamma > 1$, counterions will condense around the backbone of the polyelectrolyte to screen the electrostatic interaction between the two charges on the backbone[43,44]. This phenomenon was studied mostly with DNA since DNA has a Γ value around 4.1.[45–52] Ample experimental, theories and computer simulations have confirmed the ion condensation around the DNA helix, with a layer of ions extending to a thickness about 10Å from the DNA duplex.[53] Following the similar arguments, we examined the

potential ion condensation around the PEI chain at different protonation levels. This was monitored by calculating the radial distribution functions between N atoms on the PEI chains and Cl- anions when the salt concentration was set to 1M. Figure 6 presents the data along with the calculated excess Cl- anion. It is evident that when the protonation level increases beyond a point (somewhere between 0.25 to 0.5), the chain becomes highly charged and ions begin to condense around the PEI chain.

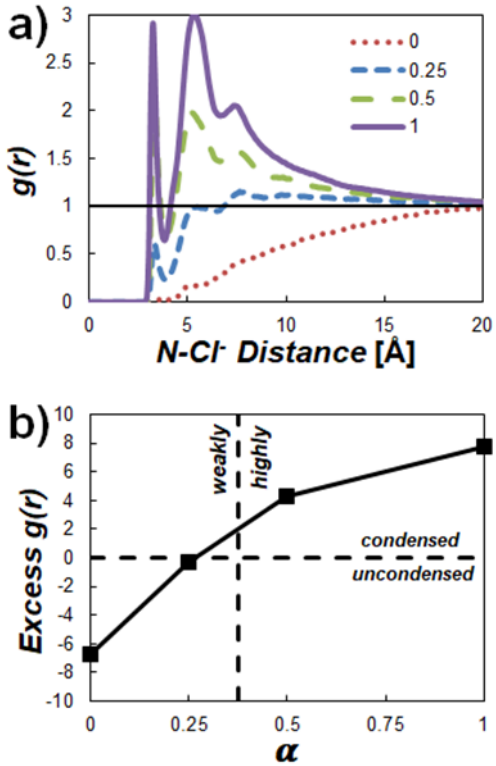

Figure 6. *(a) N-Cl⁻ radial distributions for α = 0, 0.25, 0.5 and 1.0 as shown in the figure legend with a ~1 M NaCl concentration. The α values of 0, 0.25, 0.5 and 1 are represented by the red, blue, green and purple lines respectively. (b) Excess* $g(r)$ *is defined as the integral of the radial distribution above the bulk concentration:* $\int_{2.85\,\text{Å}}^{20\,\text{Å}} g(r) - 1$*. The integration ranges from 2.85 Å, the distance of closest approach between N and Cl⁻, to 20 Å, where* $g(r)$ *approaches 1, the bulk ion density, for all protonation states. Reproduced with permission from reference [41]. Copyright [2019], American Chemical Society*

One can estimate the value of α that marks the transition from weakly charged regime to strongly charged regime by setting Γ=1. This would make the charge-to-charge distance A = l_B=7.1Å. Since A=L_0/α, one can obtain α =L_0/l_B=0.44 where we have used L_0=3.1 Å as a lower estimate for α. This level of protonation is the expected value when the solution pH=7. Therefore, one can conclude that PEI chains are in the weakly charged regime at physiological pH. Upon lowering the pH, PEI chains will pick up more protons, become

highly charged and experience a coil-to-rod conformation transition, and at the same time counter ions are condensed around the PEI rods.

Emerged Physical Picture of Potential PEI Actions during Delivery

An examination of PEI from a polymer physics perspective, by making use of molecular modeling, reveals the following physical picture on PEI actions during gene delivery. At neutral pH=7, approximately half or slightly less than half of the amine groups on PEI chains are protonated. This renders an overall positively charged polyelectrolyte that can condense negatively charged nucleic acids. If approximately half of the PEI amines are protonated, an N/P ratio near 2 would neutralize the charge of the DNA, and N/P ratios of 3 or higher would have the total charge of PEI exceeding that of the DNA. These additional PEI chains, which have been shown to enhance transfection efficiency dramatically, are believed to be free in solution and unassociated with the polyplex [28,30,54] This discussion assumes that the protonation of PEI in solution is similar to its protonation in a polyelectrolyte complex. However, this may not be the case, as experiments[55] and simulations[38], have indicated that binding to a polyanion increases PEI protonation, making it even more likely that many PEI at high N/P ratios are free in solution.

The formed polyplex, along with additional free PEI chains, likely enters the cell through endocytosis and hence remains in the endosome initially. As the endosome turns to a lysosome, the pH inside decreases. The PEI chains, free or associated with DNA, can pick up more protons pumped in by the ATPase, which could facilitate the escape from endosome and release of DNA from the polyplex. Several things could happen during this process. First, as we have discussed, PEI chains experience a coil-to-rod conformational transition when the protonation level increases. For PEI chains associated with DNA, this conformational change likely impacts the number and type of direct interactions between the DNA and the PEI, a behavior that has been observed in simulations of interactions between DNA and PEI chains with different protonation states.[56] Second, we see that ions condense around the PEI chains, especially those free, unassociated with DNA, and maybe to a lesser degree for PEI chains associated with DNA. These ions could impact both DNA-PEI interactions by screening the electrostatic attraction between DNA and free or loosely bound PEI and the development of the endosome by shifting the balance of its ionic environment[57]. All these processes occur because of the proximity of amine groups along the backbone of PEI chains. No other polycation bear similar structural characteristic as PEI. This could perhaps explain why PEI was recognized as the gold-standard in non-viral based gene delivery vectors.

The above discussion did not explore the difference between branched PEI (bPEI) and linear PEI. The change in protonation upon lowering the pH and the subsequently ion condensation around the backbone are likely to occur for branched PEI, although the coil-to-rod conformational transition will no longer occur. A recent molecular dynamic simulation of branched PEI observed that though the overall size of bPEI did not change as the protonation level increase, the overall chain becomes more elongated.[58] The actual actions of PEI on the delivery of nucleic acids need to be examined within the cellular processes. High resolution confocal microscopy studies are capable of filling the missing information.[33,34]

References

[1] Wirth, T.; Parker, N.; Ylä-Herttuala, S. History of Gene Therapy. *Gene* **2013**, *525*, 162–169.

[2] Check, E. A Tragic Setback. *Nature* **2002**, *420*, 116–118.

[3] Niidome, T.; Huang, L. Gene Therapy Progress and Prospects: Nonviral Vectors. *Gene Ther.* **2002**, *9*, 1647–1652.

[4] Schaffert, D.; Wagner, E. Gene Therapy Progress and Prospects: Synthetic Polymer-Based Systems. *Gene Ther.* **2008**, *15*, 1131–1138.

[5] Park, T. G.; Jeong, J. H.; Kim, S. W. Current Status of Polymeric Gene Delivery Systems. *Adv. Drug Deliv. Rev.* **2006**, *58*, 467–486.

[6] Lächelt, U.; Wagner, E. Nucleic Acid Therapeutics Using Polyplexes: A Journey of 50 Years (and Beyond). *Chem. Rev.* **2015**, *115*, 11043–11078.

[7] Boussif, O.; Lezoualc'h, F.; Zanta, M. A.; Mergny, M. D.; Scherman, D.; Demeneix, B.; Behr, J. P. A Versatile Vector for Gene and Oligonucleotide Transfer into Cells in Culture and in Vivo: Polyethylenimine. *Proc. Natl. Acad. Sci.* **1995**, *92*, 7297–7301.

[8] Jeong, J. H.; Kim, S. W.; Park, T. G. Molecular Design of Functional Polymers for Gene Therapy. *Prog. Polym. Sci.* **2007**, *32*, 1239–1274.

[9] Tang, M. X.; Redemann, C. T.; Szoka, F. C. In Vitro Gene Delivery by Degraded Polyamidoamine Dendrimers. *Bioconjug. Chem.* **1996**, *7*, 703–714.

[10] Midoux, P.; Breuzard, G.; Gomez, J. P.; Pichon, C. Polymer-Based Gene Delivery: A Current Review on the Uptake and Intracellular Trafficking of Polyplexes. *Curr. Gene Ther.* **2008**, *8*, 335–352.

[11] O'Rorke, S.; Keeney, M.; Pandit, A. Non-Viral Polyplexes: Scaffold Mediated Delivery for Gene Therapy. *Prog. Polym. Sci.* **2010**, *35*, 441–458.

[12] Zhu, L.; Mahato, R. I. Lipid and Polymeric Carrier-Mediated Nucleic Acid Delivery. *Expert Opin. Drug Deliv.* **2010**, *7*, 1209–1226.

[13] Du, F.-S.; Wang, Y.; Zhang, R.; Li, Z.-C. Intelligent Nucleic Acid Delivery Systems Based on Stimuli-Responsive Polymers. *Soft Matter* **2010**, *6*, 835–848.

[14] Wagner, E. Polymers for SiRNA Delivery: Inspired by Viruses to Be Targeted, Dynamic, and Precise. *Acc. Chem. Res.* **2012**, *45*, 1005–1013.

[15] Jäger, M.; Schubert, S.; Ochrimenko, S.; Fischer, D.; Schubert, U. S.; Jager, M.; Schubert, S.; Ochrimenko, S.; Fischer, D.; Schubert, U. S. Branched and Linear Poly(Ethylene Imine)-Based Conjugates: Synthetic Modification, Characterization, and Application. *Chem. Soc. Rev.* **2012**, *41*, 4755.

[16] Brissault, B.; Kichler, A.; Guis, C.; Leborgne, C.; Danos, O.; Cheradame, H. Synthesis of Linear Polyethylenimine Derivatives for DNA Transfection. *Bioconjug. Chem.* **2003**, *14*, 581–587.

[17] Tauhardt, L.; Kempe, K.; Knop, K.; Altuntaş, E.; Jäger, M.; Schubert, S.; Fischer, D.; Schubert, U. S. Linear Polyethyleneimine: Optimized Synthesis and Characterization - On the Way to "Pharmagrade" Batches. *Macromol. Chem. Phys.* **2011**, *212*, 1918–1924.

[18] Behr, J. P. The Proton Sponge: A Trick to Enter Cells the Viruses Did Not Exploit. *Chimia (Aarau).* **1997**, *51*, 34–36.

[19] Pollard, H.; Remy, J. S.; Loussouarn, G.; Demolombe, S.; Behr, J. P.; Escande, D. Polyethylenimine but Not Cationic Lipids Promotes Transgene Delivery to the Nucleus in Mammalian Cells. *J. Biol. Chem.* **1998**, *273*, 7507–7511.

[20] Godbey, W. T.; Wu, K. K.; Mikos, A. G. Tracking the Intracellular Path of

Poly(Ethylenimine)/DNA Complexes for Gene Delivery. *Proc. Natl. Acad. Sci. U. S. A.* **1999**, *96*, 5177–5181.

[21] Remy-Kristensen, A.; Clamme, J. P.; Vuilleumier, C.; Kuhry, J. G.; Mely, Y. Role of Endocytosis in the Transfection of L929 Fibroblasts by Polyethylenimine/DNA Complexes. *Biochim. Biophys. Acta, Biomembr.* **2001**, *1514*, 21–32.

[22] Forrest, M. L.; Pack, D. W. On the Kinetics of Polyplex Endocytic Trafficking: Implications for Gene Delivery Vector Design. *Mol. Ther.* **2002**, *6*, 57–66.

[23] Sonawane, N. D.; Szoka Jr., F. C.; Verkman, A. S. Chloride Accumulation and Swelling in Endosomes Enhances DNA Transfer by Polyamine-DNA Polyplexes. *J. Biol. Chem.* **2003**, *278*, 44826–44831.

[24] Funhoff, A. M.; van Nostrum, C. F.; Koning, G. A.; Schuurmans-Nieuwenbroek, N. M. E.; Crommelin, D. J. A.; Hennink, W. E. Endosomal Escape of Polymeric Gene Delivery Complexes Is Not Always Enhanced by Polymers Buffering at Low PH. *Biomacromolecules* **2004**, *5*, 32–39.

[25] Akinc, A.; Thomas, M.; Klibanov, A. M.; Langer, R. Exploring Polyethylenimine-Mediated DNA Transfection and the Proton Sponge Hypothesis. *J. Gene Med.* **2005**, *7*, 657–663.

[26] Ho, Y. P.; Chen, H. H.; Leong, K. W.; Wang, T. H. Evaluating the Intracellular Stability and Unpacking of DNA Nanocomplexes by Quantum Dots-FRET. *J. Control. Release* **2006**, *116*, 83–89.

[27] Cheng, J. J.; Zeidan, R.; Mishra, S.; Liu, A.; Pun, S. H.; Kulkarni, R. P.; Jensen, G. S.; Bellocq, N. C.; Davis, M. E. Structure - Function Correlation of Chloroquine and Analogues as Transgene Expression Enhancers in Nonviral Gene Delivery. *J. Med. Chem.* **2006**, *49*, 6522–6531.

[28] Dai, Z. J.; Gjetting, T.; Mattebjerg, M. A.; Wu, C.; Andresen, T. L. Elucidating the Interplay between DNA-Condensing and Free Polycations in Gene Transfection through a Mechanistic Study of Linear and Branched PEI. *Biomaterials* **2011**, *32*, 8626–8634.

[29] Yue, Y.; Jin, F.; Deng, R.; Cai, J.; Chen, Y.; Lin, M. C. M.; Kung, H.-F.; Wu, C. Revisit Complexation between DNA and Polyethylenimine — Effect of Uncomplexed Chains Free in the Solution Mixture on Gene Transfection. *J. Control. Release* **2011**, *155*, 67–76.

[30] Yue, Y.; Jin, F.; Deng, R.; Cai, J.; Dai, Z.; Lin, M. C. M.; Kung, H.-F.; Mattebjerg, M. A.; Andresen, T. L.; Wu, C. Revisit Complexation between DNA and Polyethylenimine — Effect of Length of Free Polycationic Chains on Gene Transfection. *J. Control. Release* **2011**, *152*, 143–151.

[31] Liang, W.; W. Lam, J. K. Endosomal Escape Pathways for Non-Viral Nucleic Acid Delivery Systems. In *Molecular Regulation of Endocytosis*; Ceresa, B., Ed.; InTech: London, UK, 2012; pp 429–456.

[32] Benjaminsen, R. V.; Mattebjerg, M. A.; Henriksen, J. R.; Moghimi, S. M.; Andresen, T. L. The Possible "Proton Sponge " Effect of Polyethylenimine (PEI) Does Not Include Change in Lysosomal PH. *Mol. Ther.* **2013**, *21*, 149–157.

[33] Vermeulen, L. M. P.; Brans, T.; Samal, S. K.; Dubruel, P.; Demeester, J.; De Smedt, S. C.; Remaut, K.; Braeckmans, K. Endosomal Size and Membrane Leakiness Influence Proton Sponge-Based Rupture of Endosomal Vesicles. *ACS Nano* **2018**, *12*, 2332–2345.

[34] Wojnilowicz, M.; Glab, A.; Bertucci, A.; Caruso, F.; Cavalieri, F. Super-Resolution Imaging of Proton Sponge-Triggered Rupture of Endosomes and Cytosolic Release of Small Interfering RNA. *ACS Nano* **2019**, *13*, 187–202.

[35] Won, Y.-Y.; Sharma, R.; Konieczny, S. F. Missing Pieces in Understanding the Intracellular Trafficking of Polycation/DNA Complexes. *J. Control. Release* **2009**, *139*, 88–93.
[36] Vermeulen, L. M. P.; De Smedt, S. C.; Remaut, K.; Braeckmans, K. The Proton Sponge Hypothesis: Fable or Fact? *Eur. J. Pharm. Biopharm.* **2018**, *129*, 184–190.
[37] Bencini, A.; Bianchi, A.; Garcia-Espana, E.; Micheloni, M.; Ramirez, J. A. Proton Coordination by Polyamine Compounds in Aqueous Solution. *Coord. Chem. Rev.* **1999**, *188*, 97–156.
[38] Ziebarth, J. D.; Wang, Y. Understanding the Protonation Behavior of Linear Polyethylenimine in Solutions through Monte Carlo Simulations. *Biomacromolecules* **2010**, *11*, 29–38.
[39] Smits, R. G.; Koper, G. J. M.; Mandel, M. The Influence of Nearest- and next-Nearest-Neighbor Interactions on the Potentiometric Titration of Linear Poly(Ethylenimine). *J. Phys. Chem.* **1993**, *97*, 5745–5751.
[40] Curtis, K. A.; Miller, D.; Millard, P.; Basu, S.; Horkay, F.; Chandran, P. L. Unusual Salt and PH Induced Changes in Polyethylenimine Solutions. *PLoS One* **2016**, *11*, e0158147.
[41] Gallops, C. E.; Yu, C.; Ziebarth, J. D.; Wang, Y. Effect of the Protonation Level and Ionic Strength on the Structure of Linear Polyethyleneimine. *ACS Omega* **2019**, *4*, 7255–7264.
[42] Teraoka, I. Wormlike Chains. In *Polymer Solutions*; Wiley: New York, 2002; pp 43–47.
[43] Manning, G. S. Limiting Laws and Counterion Condensation in Polyelectrolyte Solutions. 7. Electrophoretic Mobility and Conductance. *J. Phys. Chem.* **1981**, *85*, 1506–1515.
[44] Manning, G. S. Limiting Laws and Counterion Condensation in Polyelectrolyte Solutions I. Colligative Properties. *J. Chem. Phys.* **1969**, *51*, 924–933.
[45] Feig, M.; Pettitt, B. M. Sodium and Chlorine Ions as Part of the DNA Solvation Shell. *Biophys. J.* **1999**, *77*, 1769–1781.
[46] Deserno, M.; Holm, C.; May, S. Fraction of Condensed Counterions around a Charged Rod: Comparison of Poisson-Boltzmann Theory and Computer Simulations. *Macromolecules* **2000**, *33*, 199–206.
[47] Korolev, N.; Lyubartsev, A. P.; Laaksonen, A.; Nordenskiold, L.; Laadsonen, A.; Nordensklold, L. On the Competition between Water, Sodium Ions, and Spermine in Binding to DNA: A Molecular Dynamics Computer Simulation Study. *Biophys. J.* **2002**, *82*, 2860–2875.
[48] Zinchenko, A. A.; Yoshikawa, K. Na+ Shows a Markedly Higher Potential than K+ in DNA Compaction in a Crowded Environment. *Biophys. J.* **2005**, *88*, 4118–4123.
[49] Ponomarev, S. Y.; Thayer, K. M.; Beveridge, D. L. Ion Motions in Molecular Dynamics Simulations on DNA. *Proc. Natl. Acad. Sci. U. S. A.* **2004**, *101*, 14771–14775.
[50] Savelyev, A.; Papoian, G. A. Electrostatic, Steric, and Hydration Interactions Favor Na+ Condensation around DNA Compared with K+. *J. Am. Chem. Soc.* **2006**, *128*, 14506–14518.
[51] Bai, Y.; Greenfeld, M.; Travers, K. J.; Chu, V. B.; Lipfert, J.; Doniach, S.; Herschlag, D. Quantitative and Comprehensive Decomposition of the Ion Atmosphere around Nucleic Acids. *J. Am. Chem. Soc.* **2007**, *129*, 14981–14988.
[52] Kirmizialtin, S.; Silalahi, A. R. J.; Elber, R.; Fenley, M. O. The Ionic Atmosphere

around A-RNA: Poisson-Boltzmann and Molecular Dynamics Simulations. *Biophys. J.* **2012**, *102*, 829–838.
[53] Robbins, T. J.; Ziebarth, J. D.; Wang, Y. Comparison of Monovalent and Divalent Ion Distributions around a DNA Duplex with Molecular Dynamics Simulation and a Poisson-Boltzmann Approach. *Biopolymers* **2014**, *101*, 834–848.
[54] Clark, S. R.; Lee, K. Y.; Lee, H.; Khetan, J.; Kim, H. C.; Choi, Y. H.; Shin, K.; Won, Y.-Y. Determining the Effects of PEI Adsorption on the Permeability of 1,2-Dipalmitoylphosphatidylcholine/Bis(Monoacylglycero)Phosphate Membranes under Osmotic Stress. *Acta Biomater.* **2018**, *65*, 317–326.
[55] Lee, H.; Son, S. H.; Sharma, R.; Won, Y.-Y. A Discussion of the PH-Dependent Protonation Behaviors of Poly(2-(Dimethylamino)Ethyl Methacrylate) (PDMAEMA) and Poly(Ethylenimine- Ran -2-Ethyl-2-Oxazoline) (P(EI- r -EOz)). *J. Phys. Chem. B* **2011**, *115*, 844–860.
[56] Ziebarth, J.; Wang, Y. Molecular Dynamics Simulations of DNA-Polycation Complex Formation. *Biophys. J.* **2009**, *97*, 1971–1983.
[57] Scott, C. C.; Gruenberg, J. Ion Flux and the Function of Endosomes and Lysosomes: PH Is Just the Start: The Flux of Ions across Endosomal Membranes Influences Endosome Function Not Only through Regulation of the Luminal PH. *BioEssays* **2011**, *33*, 103–110.
[58] Kim, I.; Pascal, T. A.; Park, S.-J.; Diallo, M.; Goddard III, W. A.; Jung, Y. PH-Dependent Conformations for Hyperbranched Poly(Ethylenimine) from All-Atom Molecular Dynamics. *Macromolecules* **2018**, *51*, 2187–2194.